JOURNAL OF SOLID STATE CHEMISTRY 52, 130–137 (1984)

Luminescence in $NaLn(SO_4)_2H_2O$: A Host Lattice with High-Energy Vibrations

HAO ZHIRAN,[1] G. J. DIRKSEN, AND G. BLASSE

Physical Laboratory, State University, P.O. Box 80.000, 3508 TA Utrecht, The Netherlands

Received September 21, 1983; in revised form October 24, 1983

The luminescence of Ce^{3+}, Sm^{3+}, Eu^{3+}, Gd^{3+}, Tb^{3+}, and Dy^{3+} in $NaLn(SO_4)_2H_2O$ (Ln = lanthanide) is reported. Only Ce^{3+}, Gd^{3+}, and Tb^{3+} show efficient emission. This is explained in terms of an energy-gap law. Energy transfer is studied in several codoped compositions. The mutual transfer between Gd^{3+} ions is the only one encountered with high probability. The several transfers are discussed and where possible their rates are calculated.

1. Introduction

The crystal structure of $NaCe(SO_4)_2H_2O$ has been described by Lindgren (*1*); this composition exists for all lanthanides (*2*). The lanthanide site symmetry is C_2. Each Ln^{3+} ion is coordinated to 8 SO_4^{2-} ions and to one H_2O molecule. In the case of Ce^{3+} there are four nearest Ce^{3+} neighbors at 5.6 Å, two at 6.7 Å, and an additional six at 7.0 Å.

Brewer and Nicol (*3*) have reported on the luminescence of Ce^{3+} in Na(La,Ce)$(SO_4)_2H_2O$ and on the energy transfer from Ce^{3+} to Nd^{3+}, Ho^{3+}, and Er^{3+}. Since the water molecule with its high vibrational frequencies is coordinated directly to the Ln^{3+} ion, it seemed of interest to investigate the luminescence of several lanthanide ions in this lattice. From studies on the luminescence of lanthanide ions in aqueous solution, it is well established that the water molecule can have a fatal influence on their luminescence efficiency (see, e.g., Ref. (*4*)). The present host lattice is felt to bridge the gap between studies of lanthanide ions in aqueous solution and in solid host lattices.

Efficient luminescence was observed only for Ce^{3+}, Gd^{3+}, and Tb^{3+} in this host lattice; we also studied energy transfer processes among these ions. Transfer between these ions forms the basis for a new class of efficient lamp phosphors, which have been reported in the recent literature (*5–7*).

2. Experimental

Samples were prepared as described in the literature (*1–3*). They were checked by X-ray powder diffraction. In spite of the low preparation temperature (boiling solution), the diffraction patterns consist of sharp lines; no impurities could be detected.

The optical instrumentation is the same

[1] On leave from Changchun Institute of Physics, Chinese Academy of Sciences, Changchun, P.R. China.

0022-4596/84 $3.00

as described before (*7*) and consists essentially of a Perkin–Elmer spectrofluorometer MPF-3 equipped with an Oxford flow cryostat for measurements at liquid-helium temperature (LHeT). Quantum efficiencies were estimated by comparing the samples with standard phosphors as described elsewhere (*8*). Diffuse reflection spectra were measured on a Perkin–Elmer spectrometer EPS-3T, and infrared spectra on a Perkin–Elmer spectrometer EPI-G3.

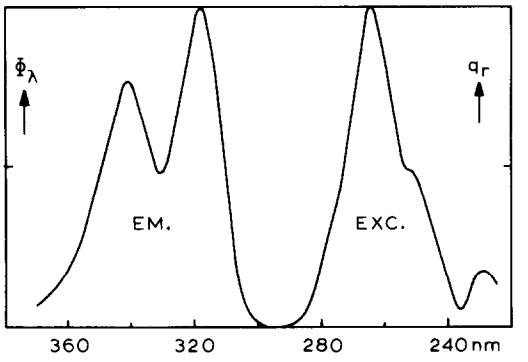

FIG. 1. Excitation (right-hand side) and emission spectra (left-hand side) of the luminescence of $NaLa_{0.95}Ce_{0.05}(SO_4)_2H_2O$ at liquid-helium temperature. Φ_λ specifies the spectral radiant power per constant wavelength interval and q_r, the relative quantum output in arbitrary units.

3. Results and Discussion

3.1. The Ce^{3+} Ion

In agreement with the results of Ref. (*3*) the Ce^{3+} ion shows efficient luminescence in $NaLa(SO_4)_2H_2O$. Here we present some additional information. Our spectra, especially those at LHeT, show considerably more detail than those in Ref. (*3*). The emission band is clearly a double peak, as shown in Fig. 1. The energy difference between the two maxima is about 2100 cm^{-1}, which corresponds to the energy difference between the ground-state levels $^2F_{7/2}$ and $^2F_{5/2}$ (2200 cm^{-1}).

The excitation spectrum of this emission is also shown in Fig. 1. We observed at least four bands, viz. at ~34,000, 37,800, ~40,000, and ~43,500 cm^{-1}. The total splitting of some 10,000 cm^{-1} agrees well with earlier results in the literature, although usually somewhat larger values are reported (*9*). This splitting presents the crystal-field splitting of the excited 5*d* level of the Ce^{3+} ion. In view of the C_2 site symmetry five bands are expected. The fifth component can be easily overlooked in this spectral region: the bands are broad and the spectrometer is rather insensitive, due to the low output of the light source (Xe lamp).

The quantum efficiency of the Ce^{3+} emission was found to be high at 300 K and below (~80%). In Ref. (*3*) a decay time of 21 ns has been reported which shows, in view of the high quantum efficiency, that emission is due to an allowed transition (5*d* → 4*f*).

One should note, in Fig. 1, the absence of a sizeable spectral overlap between the emission and excitation spectra. We were able to reproduce the result of Ref. (*3*) that the Ce^{3+} luminescence in $NaLa(SO_4)_2H_2O$ is not subject to concentration quenching. We ascribe this fact to the small spectral overlap which leads to a low transfer probability, especially if one considers the large distance (5.6 Å) between the Ce^{3+} ions (*10*).

In summary, the Ce^{3+} ion exhibits efficient luminescence in $NaLa(SO_4)_2H_2O$. This luminescence is not liable to temperature quenching (up to room temperature) nor concentration quenching. The efficiency is not influenced by water molecules.

3.2. The Gd^{3+} Ion

The Gd^{3+} ion gives rise to efficient ultraviolet emission in the host lattice $NaLa(SO_4)_2H_2O$. The emission corresponds to the $^6P \rightarrow {}^8S$ transition. The excitation peaks correspond to $^8S \rightarrow {}^6P$, ^6I, ^6D (see, e.g.,

Ref. (*11*)). AT liquid-helium temperatures the emission spectrum consists of the $^6P_{7/2} \rightarrow {}^8S$ transition, accompanied by a weak line at ~1150 cm^{-1} lower energy. Its intensity is a few percent of that of the $^6P_{7/2} \rightarrow {}^8S$ line. The weak line is ascribed to a vibronic transition due to coupling of the electronic transition on the Gd^{3+} ion with the SO_4^{2-} stretching vibration (*12*). At room temperature, the emission spectrum also involves the $^6P_{5/2} \rightarrow {}^8S$ transition. The quantum efficiency of the Gd^{3+} emission is estimated to be near 100% at 300 K and at lower temperatures. No temperature quenching was observed for dilute Gd^{3+} compositions. At liquid-helium temperature no concentration quenching of the Gd^{3+} emission was observed. This does not necessarily mean that energy transfer between Gd^{3+} ions is absent. It has been shown that energy transfer between Gd^{3+} ions may be very efficient, even down to low temperatures (*13*). However, due to perturbations, the energy difference between the excited state and the ground state varies from ion to ion. This hampers energy migration at very low temperatures, the resonance condition then being no longer fulfilled (see, e.g., Ref. (*14*)). Energy migration among the Gd^{3+} sublattice is more easily followed using an efficient luminescent trap, as will be discussed below.

3.3. The Tb^{3+} Ion

The Tb^{3+} ion gives rise to an efficient, green luminescence in $NaLa(SO_4)_2H_2O$. Even for the lowest Tb^{3+} concentration (~0.01 m/o) no $^5D_3$ emission could be observed. The emission originates only from the $^5D_4$ state. This shows that the rate of nonradiative $^5D_3 \rightarrow {}^5D_4$ relaxation is considerably larger than the $^5D_3 \rightarrow {}^7F_J$ radiative rate. Since the $^5D_3$–$^5D_4$ energy difference is rather large (5500 cm^{-1}), the high nonradiative rate points to a role in this process played by the water or sulfate constituents. Similar observations were reported for $(Y,Tb)Al_3B_4O_{12}$ (Ref. (*15*)).

In Fig. 2 the excitation spectrum of the emission of $NaTb(SO_4)_2H_2O$ is presented. These lines correspond to the well-known transitions in the $4f^8$ Tb^{3+} subshell (*11*). With the present instrumentation we could not observe the $4f \rightarrow 5d$ transitions; thus, they must be situated at $\lambda < 240$ nm. The quantum efficiency for excitation into the Tb^{3+} lines is about 70% at 300 K and at lower temperatures. In the system $Na(La,Tb)(SO_4)_2H_2O$ we observed neither temperature quenching nor concentration quenching, showing that this system is comparable with $(Y,Tb)Al_3B_4O_{12}$ (Ref. (*15*)).

If $NaGd(SO_4)_2H_2O$ is used as a host lattice instead of $NaLa(SO_4)_2H_2O$, the results are only different for excitation into the Gd^{3+} ions. For this purpose we used the $^8S \rightarrow {}^6I$ transition, which is the stronger Gd^{3+} transition, and permits observation of the Gd^{3+} emission ($^6P \rightarrow {}^8S$). As will be discussed below, the total $Gd^{3+} \rightarrow Tb^{3+}$ transfer is by no means complete, not even at room temperature.

3.4. The Eu^{3+} Ion

The luminescence efficiency of the Eu^{3+}

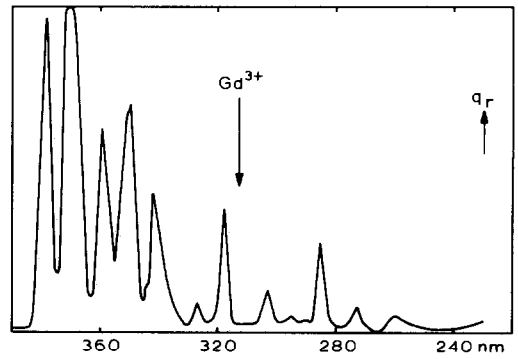

FIG. 2. Excitation spectrum of the emission of $NaTb(SO_4)_2H_2O$ at liquid-helium temperature. The arrow marked Gd^{3+} indicates the emission line maximum of Gd^{3+} (see text).

ion in $NaLa(SO_4)_2H_2O$ and $NaGd(SO_4)_2H_2O$ is low, even at liquid-helium temperature. The quantum efficiency was estimated to be about 10%. Figure 3 presents the emission spectrum at liquid-He temperature. Emission is only observed from the lowest ^5D level, similar to the observations for Tb^{3+}. The site symmetry of the Eu^{3+} ion (C_2) involves complete splitting of all energy levels and all possible transitions between them. From Fig. 3, it is clear that this situation is not encountered under our experimental conditions: $^5D_0$–$^7F_0$ is not observed, $^5D_0$–$^7F_1$ is split into a broader and a narrower line, and $^5D_0$–$^7F_2$ is not clearly split. Measurements under higher resolving power might improve our result, but it is nevertheless clear that the total crystal-field splitting is relatively small. This agrees with the results for Ce^{3+} reported above.

In Fig. 4 the excitation spectrum of the Eu^{3+} emission is presented. In addition to the excitation lines, due to transitions in the $4f^7$ subshell, a broad charge-transfer excitation band is present. Its maximum is situated at relatively high energy, viz. about 40,500 cm^{-1}. At room temperature, its position is at about 38,500 cm^{-1}, in reasonable agreement with a strong absorption band in the diffuse reflection spectrum peaking at about 41,500 cm^{-1} (the instrumental inaccuracy in this region is large). Nonradiative

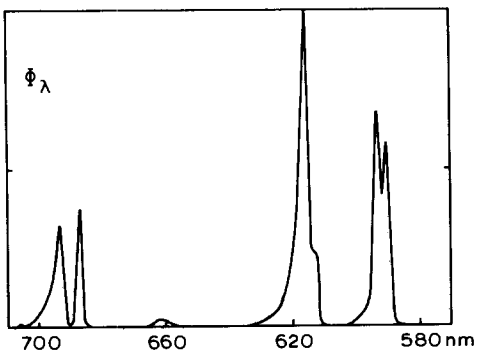

FIG. 3. Emission spectrum of $NaEu(SO_4)_2H_2O$ at liquid-helium temperature.

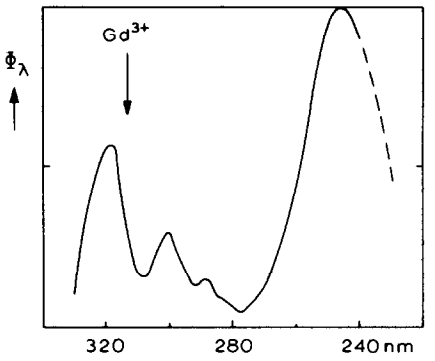

FIG. 4. Excitation spectrum of the emission of $NaEu(SO_4)_2H_2O$ at liquid-helium temperature. Due to the low emission intensity, the linewidth is determined by the slitwidth of the spectrometer. The short wavelength side of the charge-transfer band is rather inaccurate. The arrow marked Gd^{3+} indicates the emission line maximum of Gd^{3+} (see text).

transitions from the emitting $^5D_0$ level of the Eu^{3+} ion may occur via the charge-transfer state if it is situated at low energies. This case can be excluded for the present (*16*), so that the low quantum efficiency must be due to multiphonon emission involving the water molecule (see below).

No concentration quenching of the Eu^{3+} emission was observed in the system $NaLa_{1-x}Eu_x(SO_4)_2H_2O$.

The luminescence of the Eu^{3+} ion in $NaGd(SO_4)_2H_2O$ is similar to that in the lanthanum compound. In addition, we observed $Gd^{3+} \rightarrow Eu^{3+}$ energy transfer as described above for Tb^{3+}, and as further discussed below. In summary, the Eu^{3+} ion in $NaLn(SO_4)_2H_2O$ does show neither temperature or concentration quenching. However, at liquid-helium temperature the greater part of the excitation energy is lost nonradiatively by a temperature-independent process.

3.5. *The Sm^{3+} and Dy^{3+} Ion*

For the compositions $Na(Gd,Sm)(SO_4)_2H_2O$ and $Na(Gd,Dy)(SO_4)_2H_2O$, no Sm^{3+} or Dy^{3+} luminescence was encountered. We assume, therefore, that the quan-

tum efficiency of the luminescence of these ions is very low, i.e., $q < 1\%$.

In the previous paragraphs we have discussed the luminescence properties of the single ions in $NaLn(SO_4)_2H_2O$. We will now compare the nonradiative transitions in these ions in this host lattice (Sec. 3.6) and then the several energy transfer processes (sec. 3.6–9).

3.6 Nonradiative Transitions

The infrared spectrum of $NaLa(SO_4)_2H_2O$ was measured in order to have available the frequencies of the higher frequency vibrations. These appeared to occur at 3450 cm^{-1} (H_2O stretching), 1600 cm^{-1} (H_2O bending), 1100 cm^{-1} (SO_4^{2-} stretching), and 600 cm^{-1} (SO_4^{2-} bending).

Nonradiative transitions between the $4f$ energy levels have been studied intensively and are relatively well understood (see, e.g., Ref. (*17*)). For different lanthanide ions in one host lattice these nonradiative rates obey the so-called, energy gap law

$$k_{NR} = \beta \exp[-\alpha \cdot \Delta E],$$

where α and β are constants and ΔE is the energy gap between the levels involved. Recently Van Dijk and Schuurmans (*18*) proposed a modified exponential energy gap law for transitions, where in only a few phonons participate in the transition. Its form is given by

$$k_{NR} = \beta \exp[-(\Delta E - 2\hbar\omega_{max})\alpha] \quad (1)$$

The energy gap is reduced by two maximum phonon energies, accounting for the action of promoting modes (*16, 17*). The value of β now varies by only a factor of 10 for different host lattices. Furthermore, they were able to relate k_{NR} to k_R, the radiative rate. In this way nonradiative rates could be estimated to within one order of magnitude.

In the present case ΔE as well as $\hbar\omega_{max}$ lie far beyond the region of values studied by Van Dijk and Schuurmans. Nevertheless, their theory should cover the present case as well. Let us consider the Eu^{3+} ion with a gap ($^5D_0$–$^7F_6$) of about 12,000 cm^{-1}. The value of k_R involved is estimated to be 5×10^2 s^{-1}, assuming a radiant lifetime of the $^5D_0$ level of 0.2 ms and 10% $^5D_0$–$^7F_6$ emission in the total Eu^{3+} emission (which is probably an overestimate). In this way we find for β a value of about 10^9 s^{-1}. Since the calculated β values in Ref. (*18*) are about one order of magnitude too low, we calculated k_{NR} using $\beta = 10^{10}$ s^{-1}. With Eq. (1), and $\alpha = 4.5 \times 10^{-3}$ cm, we find k_{NR} 2 s^{-1}. This value cannot compete with the total radiative rate. Therefore we replaced the factor 2 in Eq. (1) by 2.5, the upper bound allowed in Ref. (*18*); then $k_{NR} = 4.5 \times 10^3$ s^{-1}. This is of the same order as the total radiative rate. In order to explain the low quantum efficiency of the Eu^{3+} emission in $NaLa(SO_4)_2H_2O$ with Eq. (1), we have to use a high value of β and a high reduction of the gap (viz. by the amount of 2.5 times maximum phonon energies).

With these values, we calculate for Tb^{3+} (where $\Delta E \sim 15{,}000$ cm^{-1}) a value of $k_{NR} \approx 10^{-2}$ s^{-1}, which explains the high value of the quantum efficiency. For Sm^{3+} and Dy^{3+}, very high k_{NR} values are to be expected, their gaps being considerably smaller (~7,500 cm^{-1}).

These results may be compared with those observed for lanthanide luminescence in aqueous solutions (*4*). Here it has been found that the nonradiative losses increase drastically in the sequence $Gd^{3+} < Tb^{3+} < Eu^{3+} < Sm^{3+}$, Dy^{3+}. The important role of the water molecule vibrations in the nonradiative processes becomes clear if H_2O is replaced by D_2O: the role of the nonradiative processes is reduced, because the order of the relevant multiphonon process is decreased.

Our observations parallel those in solutions. A striking difference is encountered in the case of Tb^{3+}. Our results suggest that the coordination by one water molecule in

$NaLn(SO_4)_2H_2O$ is insufficient to quench the $^5D_4$ emission, whereas the coordination by a number of water molecules in a solution considerably reduces the quantum efficiency.

The temperature dependence of the nonradiative processes under discussion is given by

$$k_{NR}(T) = k_{NR}(0)\{1 + [\exp(\hbar\omega_{max}/kT) - 1]^{-1}\}^p,$$

where $p = \Delta E/\hbar\omega_{max}$, the number of phonons involved in the process (*17*). For $\hbar\omega_{max} = 3450\ cm^{-1}$ and $T \leq$ room temperature, k_{NR} is practically temperature independent. This agrees with our experimental results.

Finally we note that Brewer and Nicol (*3*) report Nd^{3+} luminescence from Na(La, Nd)$(SO_4)_2H_2O$. In view of the decay times reported, the quantum efficiency should be in the range of several tens percent. This seems to imply that the water vibrations do not play a role in the nonradiative processes for the Nd^{3+} ion. This point deserves further attention, especially because DeShazer and coworkers have reported low quantum efficiencies for Nd^{3+} next to OH groups present as impurities in $Y_3Al_5O_{12}$ (*19*).

In summary, the water molecule in $NaLn(SO_4)_2H_2O$ is not able to quench the Gd^{3+} and Tb^{3+} luminescence. The Eu^{3+}, and particularly Sm^{3+} and Dy^{3+}, luminescences are strongly quenched, however. The Ce^{3+} case should not be discussed on the arguments given above, because the transition involved is not of the $4f - 4f$ type.

3.7. $Ce^{3+} \rightarrow Tb^{3+}$ Energy Transfer

In the system Na(*Ln*,Ce,Tb)$(SO_4)_2H_2O$, energy transfer from Ce^{3+} to Tb^{3+} was observed. The excitation spectrum of the Tb^{3+} emission contains the Ce^{3+} excitation bands. To specify this transfer process, the composition $NaCe_{0.97}Tb_{0.03}(SO_4)_2H_2O$ was investigated.

Since $Ce^{3+} \rightarrow Ce^{3+}$ transfer was shown to be absent (see above), the only possible transfer is $Ce^{3+} \rightarrow Tb^{3+}$. Upon excitation into the Ce^{3+} ion, the emission was found to consist of Ce^{3+} (90%) and Tb^{3+} (10%), independent of temperature.

In a simple model, with only $Ce^{3+} \rightarrow Tb^{3+}$ transfer between nearest neighbors, the probability for Ce^{3+} emission is 89% and for Tb^{3+} emission (after transfer) 11%; this is in excellent agreement with experiment. This calculation is based on the structure determination which indicates four nearest neighbor sites. For a 3% Tb content, the probability that Ce^{3+} has only Ce^{3+} neighbors, is $0.97^4 = 89\%$. This argument yields a critical distance (R_c) for the $Ce^{3+} \rightarrow Tb^{3+}$ transfer of 6 Å. With the relation $R_c^6 = 0.63 \times 10^{28}\ Q_A E^{-4} \int f_s(E) F_A(E) dE$, where Q_A is the absorption cross section of Tb^{3+}, and where the integral represents the spectral overlap (*20*), it is possible to calculate R_c from spectral data. With a spectral overlap of $0.5\ eV^{-1}$ from the spectra, and with $Q_A \simeq 3.5 \times 10^{-21}$ cm^2 eV as quoted in the literature (*4*), the result is $R_c = 6$ Å, in good agreement with experiment.

These results inform us that high Tb^{3+} concentrations are necessary for a more or less complete $Ce^{3+} \rightarrow Tb^{3+}$ transfer in this host lattice. This can be achieved also by using Gd^{3+} as an intermediary (*5–7*). Therefore, we studied the energy transfer between Ce^{3+} and Gd^{3+}.

3.8. $Ce^{3+} \rightarrow Gd^{3+}$ Transfer

If Ce^{3+}-activated $NaGd(SO_4)_2H_2O$ is excited into the Ce^{3+} excitation band avoiding the Gd^{3+} excitation lines as much as possible, the output for the greater part consists of the Ce^{3+} emission. For $NaGd_{0.95}Ce_{0.05}(SO_4)_2H_2O$, the amount of Ce^{3+} emission amounts to 75%. The amount of Gd^{3+}

emission is less (25%). These figures are valid for liquid-helium temperature; at room temperature they are different, viz. 95 and 5%, respectively. Since the Ce^{3+} content is only a few mole percent, nearly every Ce^{3+} has only Gd^{3+} neighbors. We conclude that $Ce^{3+} \rightarrow Gd^{3+}$ transfer cannot compete with the Ce^{3+} radiative emission. Since the $Ce^{3+} \rightarrow Gd^{3+}$ transfer can be efficient in other lattices (*5–7*), and the spectral overlap integral is not too unfavorable in the present host lattice, the Ce^{3+}–Gd^{3+} distance is not short enough. The Gd^{3+} absorption (~313 nm) overlaps the Ce^{3+} emission band in the high-energy side only (Fig. 1). The spectral overlap is equal to about 2.0 eV^{-1}, and $Q_A(Gd^{3+})$, to about 10^{-22} cm^2 eV. This yields a value of $R_c \simeq 4.2$ Å, which excludes an important contribution to $Ce^{3+} \rightarrow Gd^{3+}$ transfer by electric dipole–dipole interaction, in view of the shortest possible Ce^{3+}–Gd^{3+} distance (about 5.5 Å). Contributions by exchange interaction must be small as well. The amount of Gd^{3+} emission at LHeT by electric dipole–dipole interaction alone is estimated to be $(4.2/5.5)^6 = 0.20$, which agrees satisfactorily with the experimental value.

At room temperature, the Ce^{3+} absorption spectrum has broadened and shifted to lower energies (*3*). As a consequence, back transfer from Gd^{3+} to Ce^{3+} becomes possible. With $Q_A(Ce^{3+}) = 5 \times 10^{-18}$ cm^2 eV (*20*) and with the experimentally found spectral overlap (0.10 eV^{-1}), R_c is estimated to be 10 Å, which is much larger than the shortest Gd^{3+}–Ce^{3+} distance. This large value is mainly due to the high oscillator strength on the Ce^{3+} ion (allowed transition). This value of R_c yields $(10/5.5)^6.2\times 10^3$ $s^{-1} = 8.10^4$ s^{-1} for the $Gd^{3+} \rightarrow Ce^{3+}$ transfer rate at a 5.5-Å separation.

This back-transfer process has to compete with another process, viz. the $Gd^{3+} \rightarrow Gd^{3+}$ transfer, which, at room temperature occurs at rates of 10^5–10^7 s^{-1} (*7*). The excitation energy transferred from Ce^{3+} to Gd^{3+} is, therefore, not immediately back transferred. First, it migrates among the Gd^{3+} sublattice during which migration the Gd^{3+} radiative rate competes with the $Gd^{3+} \rightarrow Ce^{3+}$ back-transfer rate. Since the spectral overlap for $Ce^{3+} \rightarrow Gd^{3+}$ transfer does not change much with temperature, 20% of the Ce^{3+} excitation energy is transferred to the Gd^{3+} sublattice. If the transfer in that sublattice is fast enough, this migration is of the fast-diffusion type. Neglecting the back-transfer process for this 20% the Gd^{3+}/Ce^{3+} emission ratio due to this 20% equals $20 \times 2 \times 10^3/8 \times 10^4 = 0.5$. Here, 20 is the concentration ratio of Gd^{3+} and Ce^{3+}. This means that about 7% of the emission should involve the Gd^{3+} ion and 93% the Ce^{3+} ion. In view of the inaccuracies, the agreement with the experimental value is good. This result excludes the possibility that efficient phosphors might be made from $Na(Gd,Ce,Tb)(SO_4)_2H_2O$, which fact was confirmed by experiment.

3.9. *$Gd^{3+} \rightarrow Tb^{3+}$, Eu^{3+} Transfer*

As reported above samples with composition $NaGd_{1-x}R_x(SO_4)_2H_2O$ (R = Eu,Tb) undergo energy transfer from the Gd^{3+} ion to Eu^{3+} or Tb^{3+}. If these samples are excited in the $^8S \rightarrow {}^6I$ transition of the Gd^{3+} ion (~277 nm), the emission at liquid-helium temperature consists mainly of Gd^{3+} emission ($^6P \rightarrow {}^8S$), viz. >90%; the emission at room temperature, however, consists of Gd^{3+} and Eu^{3+} or Tb^{3+} emission as well. The amount of Eu^{3+} emission is about 40% of the total emission; the amount of Tb^{3+} emission is about 70% of the total emission. These figures relate to samples with $x = 0.03$. The results show that the total transfer from Gd^{3+} to the activator ions involved is far below 100%, in contradiction with results for other systems (*5–7, 21*).

The reason for the high Gd^{3+} output at liquid-helium temperature was discussed

above, viz., a hampering of the Gd^{3+} migration. At higher temperatures, however, the energy migration in the Gd^{3+} sublattice can be simulated by the fast diffusion model, i.e., the probability for $Gd^{3+} \rightarrow Gd^{3+}$ transfer is larger than the probability for $Gd^{3+} \rightarrow Tb^{3+}$ (Eu^{3+}) transfer (*7, 13*). The ratio of Gd^{3+} and Tb^{3+} (Eu^{3+}) emission intensities in this model is given by the ratio of the products of the concentration of Gd^{3+} and of the radiative rate of Gd^{3+}, and by the concentration of Tb^{3+} (Eu^{3+}) multiplied by the transfer rate of Gd^{3+} to Tb^{3+} (Eu^{3+}). Nonradiative losses are not considered. To obtain a value for the transfer rate from the experimental intensity ratios, a correction for the nonradiative losses in the Tb^{3+} (Eu^{3+}) ion is necessary. With the quantum efficiencies of 70% for Tb^{3+} 10% for Eu^{3+} (see above), we find that the intensity ratios Gd/Tb(Eu) in the absence of nonradiative losses would have been 0.30 for Tb^{3+}, and 0.15 for Eu^{3+}. With $x = 0.03$, the $Gd^{3+} \rightarrow Tb^{3+}$ transfer rate is found to be $2 \times 10^5\ s^{-1}$, and the $Gd^{3+} \rightarrow Eu^{3+}$ transfer rate, $4 \times 10^5\ s^{-1}$. Here the radiative Gd^{3+} rate was taken to be $2.10^3\ s^{-1}$ (*13*). The $Gd^{3+} \rightarrow Tb^{3+}$ transfer rate in $NaGd(SO_4)_2H_2O$ is smaller than, e.g., in $GdMgB_5O_{10}$, where it amounts to $4 \times 10^6\ s^{-1}$ (*7*). This difference must be mainly due to a distance effect. The shortest Gd^{3+}–Gd^{3+} distance in $GdMgB_5O_{10}$ is 4.0 Å. Assuming dipole–dipole interaction, the larger distance in $NaGd(SO_4)_2H_2O$ reduces the transfer rate by a factor of $(4.0/5.6)^6 = 0.13$. In Figs. 2 and 4, the position of the Gd^{3+} emission line has been drawn. This provides an indication of the spectral overlap involved in the $Gd^{3+} \rightarrow Tb^{3+}$ (Eu^{3+}) transfer.

In conclusion, the host lattice $NaLn(SO_4)_2H_2O$ is an interesting one for the study of nonradiative decay between $4f^n$ levels with a large energy separation. The energy transfer processes investigated here show relatively low rates; the reasons for this effect can be understood.

References

1. O. LINDGREN, *Acta Chem. Scand. Ser. A* **31,** 591 (1977).
2. L. L. ZAITSEVA, M. I. KONAREV, A. A. KRUGLOV, AND N. TCHEBOTAREV, *J. Inorg. Chem. (USSR)* **9,** 1380 (1964).
3. R. M. BREWER AND M. NICOL, *J. Lumin.* **23,** 269 (1981).
4. W. T. CARNALL, *in* "Handbook on the Physics and Chemistry of Rare Earths" (K. A. Gschneidner Jr. and Leroy Eyring, Eds.), Chap. 4, North-Holland, Amsterdam (1979).
5. J. TH. W. DE HAIR AND J. T. C. VAN KEMENADE, Paper No. 54, Third International Conference Science Technology Light Sources, Toulouse, April 1983.
6. G. BLASSE, *Phys. Status Solidi* A **73,** 205 (1982).
7. M. LESKELÄ, M. SAAKES, AND G. BLASSE, *Mater. Res. Bull.*, in press.
8. A. BRIL AND W. HOEKSTRA, *Philips Res. Rep.* **16,** 356 (1961).
9. G. BLASSE AND A. BRIL, *J. Chem. Phys.* **47,** 5139 (1967).
10. R. C. POWELL AND G. BLASSE, *Struct. Bonding (Berlin)* **42,** 43 (1981).
11. G. F. IMBUSCH AND R. KOPELMAN, *in* "Topics in Applied Physics" (W. M. Yen and P. M. Selzer, Eds.), Vol. 49, Chap. 1, Springer-Verlag, Berlin (1981).
12. D. W. HALL, S. A. BREWER, AND M. J. WEBER, *Phys. Rev. B* **25,** 2828 (1982).
13. F. KELLENDONK AND G. BLASSE, *Phys. Status Solidi* B **108,** 541 (1981).
14. T. HOLSTEIN, S. K. LYO, AND R. ORBACH, *in* "Topics in Applied Physics" (W. M. Yen and P. M. Selzer, Eds.), Vol. 49, Chap. 2, Springer-Verlag, Berlin (1981).
15. F. KELLENDONK AND G. BLASSE, *J. Phys. Chem. Solids* **43,** 481 (1982).
16. G. BLASSE, *in* "Radiationless Processes" (B. DiBartolo, Ed.), p. 287. Plenum, New York (1980).
17. F. AUZEL, in "Radiationless Processes" (B. DiBartolo, Ed.). p. 213. Plenum, New York (1980).
18. J. M. F. VAN DIJK AND M. F. H. SCHUURMANS, *J. Chem. Phys.* **78,** 5317 (1983).
19. D. P. DEVOR AND L. G. DESHAZER, *Opt. Commun.* **46,** 97 (1983); G. Blasse, *in* "Solid State Chemistry 1982" (R. Metselaar, H. J. M. Heijligers, and J. Schoonman, Eds.), p. 153, Ref. 4, Elsevier, Amsterdam (1983).
20. G. BLASSE, *Philips Res. Rep.* **24,** 131 (1969).
21. M. J. J. LAMMERS AND G. BLASSE, in press.